Accepted for presentation in: 2024 IEEE International Conference on Communications (ICC) - Workshop on Emerging Technologies in Aerial and Space Networks, Denver, Colorado, USA, June 2024.

Aerial-DRaGon: Machine Learning-based Channel Modeling for Airspace Communication Networks

Melina Geis, Tim Gebauer, Harun Tuna, and Christian Wietfeld
Communication Networks Institute, TU Dortmund University, 44227 Dortmund, Germany
e-mail:{ Melina.Geis, Tim.Gebauer, Harun.Tuna, Christian.Wietfeld}@tu-dortmund.de

***Abstract*—The planning and reliable operation of air-space networks strongly relies on accurate radio propagation modeling. In previous work, we demonstrated that the machine learning-driven DRaGon method outperforms channel prediction for both traditional empirical models as well as raytracing. With this paper, we introduce this new generation of data-driven channel models to aerial networks in which communication nodes move at different heights above the ground. For accurate and time-critical predictions, the proposed Aerial-DRaGon model considers a vast range of features, from communication-specific to geospatial and meteorological. In a comprehensive performance evaluation, the results for Aerial-DRaGon - using several lightweight machine learning algorithms - are compared against real-world measurements from diverse environments. There, it is found that gradient-boosted tree learners yield the best prediction accuracy. The best-performing regressors are further compared with a diverse set of state-of-the-art channel models for both terrestrial as well as aerial networks. As Aerial-DRaGon outperforms the latter, it proves itself as a promising channel prediction candidate for future air-space-networks applications like communication-aware trajectory planning.**

I. Introduction

Airborne systems find applications across diverse domains, ranging from search and rescue missions to being used as air taxis and for autonomous package delivery. The subgroup of Unmanned Aerial Vehicles (UAVs) stands out in particular due to their increasingly autonomous functionalities and the resulting low operating costs. Despite the emerging autonomy, it is currently essential that operators are able to intervene, requiring an Air to Ground (A2G) communication link. In addition, Air to Air (A2A) communication between flight participants is crucial for safe operation so that the UAVs rely heavily on secure and stable communication solutions. In order to meet these high demands, radio propagation models are used to allow a fundamental estimation of the channel characteristics and thus enable a forecast of the operating communication conditions along future trajectories. This is also highlighted by the 5G Automotive Association in [1].

While numerous detailed channel models exist for Ground to Ground (G2G) applications, the situation alters when extended into 3D space, as the established models are mostly limited to a maximum receiver height. Present drone-specific channel models are also primarily based on ground-based models fitted by empirical measurements, which can be error-prone and limit them to similar hardware and channel conditions. Furthermore, communication conditions in 3D space differ regarding increased Line-of-Sight (LOS) likelihood, and interference becomes more critical as the receiver might have a LOS link with more than one serving antenna [2]. Therefore, accurate channel modeling is crucial for UAV trajectory planning, their dynamic adaption, and optimization [3].

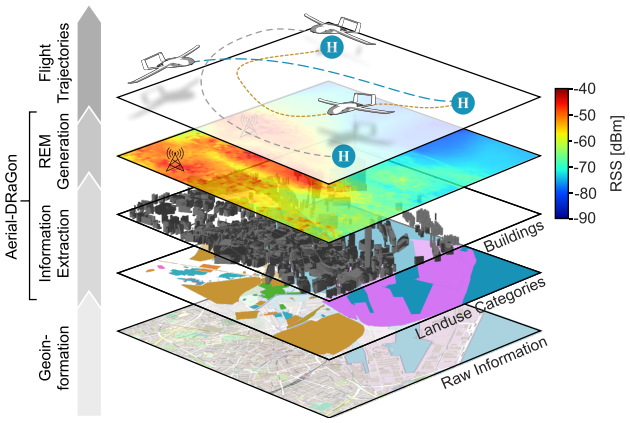

Fig. 1. Proposed channel modeling exemplarily illustrated for air taxis. Based on a scenario bounding box geospatial features are extracted in order to generate an RSS REM of the scenario. (Map data: © OpenStreetMap Contributors, CC BY-SA)

Our paper introduces a novel approach to modeling 3D channel conditions using Machine Learning (ML), incorporating geo-features of the environment and weather data to enhance propagation prediction. Our previous works [4] and [5] showed the potential of improving path loss predicition models in G2G scenarios using ML. However, these models create environmental images to utilize them in the learning process, while the proposed method goes one step further by directly extracting features from the raw geo-data to allow a reduction of the computational effort. Fig. 1 shows the proposed Aerial-DRaGon[1] on the example of cooperating air taxis, where essential information such as the geospatial data is extracted and utilized for the ML-predicted Radio Environmental Map (REM). The latter can then be used for communication-aware trajectory planning.

The remainder of this paper is structured as follows. First, the current state-of-the-art of 3D channel modeling is dis-

[1]The acronym DRaGon was created with the first version of our ML-enabled channel prediction method: Deep RAdio channel modeling from GeOinformatioN. In subsequent work, we extended the scope considerably from deep learning to other ML methods and further evolved the basis for feature engineering to include much more diverse data than geo-information. Today, we generally use the acronym DRaGon for our ML-enabled channel prediction methods, independent of its origin.

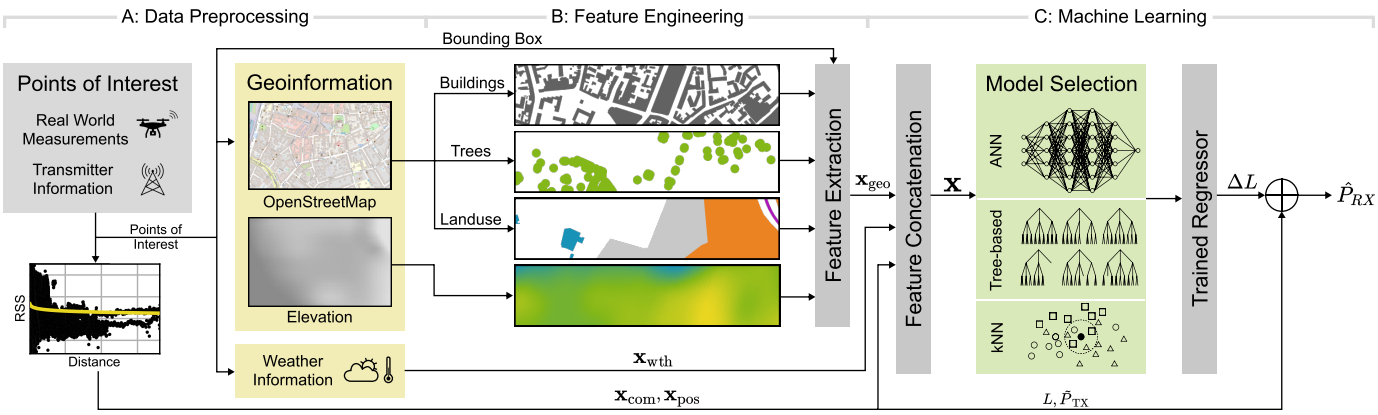

Fig. 2. Aerial-DRaGons overall system architecture. (Map data: © OpenStreetMap Contributors, CC BY-SA)

cussed in Sec. II. Then, we introduce the new Aerial-DRaGon approach in Sec. III, followed by the methodology Sec. IV. Finally, the detailed results are discussed in Sec. V.

II. Related Work

Aerial channel models are highly limited in literature and often lack cross-scenario applicability as they are based on fitted empirical data. In [6], the 3rd Generation Partnership Project (3GPP) defines channel models for various application areas (e.g. Rural Macro (RMa), Urban Macro (UMa)), but the receiver height is mainly limited to a maximum of 25 m. Therefore, in [7] 3GPP presents adapted path loss models based on a study analyzing the ability of UAVs to be served with G2G-designed Long Term Evolution (LTE) base stations. In [2] it is found that interference power increases with UAV height due to LOS likelihood, which is also confirmed by [8]. The authors also model the path loss using a log-distance model with curve-fitted parameters to the measurements in [9] as well as [2]. In contrast, [10] introduces Alpha-Beta-Gamma (ABG) parameter fitted to low altitude UAV measurements. In prior work at our institute, a simple height-dependent path loss model [11] was introduced and extended in [12] by inlcuding more antenna-related parameters.

In recent years, ML-based channel models emerged increasingly [13]. Some of them also include UAV data in their training procedure. For example, this counts for the DRaGon models proposed in [4] and [5]. These models take multiple geometry-based features as well as two distinct synthetic images of the receiver's environment into account, allowing the ML model to learn propagation effects caused by buildings and terrain.

III. Approach

Problem statement: Our goal is to retrieve a model for the calculation of the Received Signal Strength (RSS) at a specific 3D receiver position $\mathbf{p}_{\text{RX}}$ given the 3D transmitter position $\mathbf{p}_{\text{TX}}$ in an outdoor environment. For this purpose, we utilize a generic model

$$P_{\text{RX}}(\mathbf{p}_{\text{RX}}, \mathbf{p}_{\text{TX}}) = \underbrace{\tilde{P}_{\text{TX}}}_{\text{Communication system}} - \underbrace{L(\mathbf{p}_{\text{RX}}, \mathbf{p}_{\text{TX}})}_{\text{Channel model}} + \underbrace{\Delta L(\mathbf{x})}_{\text{ML-based correction}} \quad (1)$$

that estimates P_{RX} based on $\tilde{P}_{\text{TX}}$, which accumulates the transmit power and the antenna gains and losses of the receiver and transmitter. L is the path loss of an analytical radio channel model, and ΔL a correction offset. We determine L based on the UAV-specific log-distance model from [2], while ΔL is obtained using the proposed ML pipeline. The Aerial-DRaGon model is designed to accurately predict ΔL based on a feature vector $\mathbf{x}$ describing the wave's propagation environment in an A2G context. The overall system architecture of the proposed method can be seen in Fig. 2.

A. Data Preprocessing

In the context of data preprocessing, environmental data about the propagation environment is required. The primary data source for this work is Open Street Map (OSM), where the geographic data is described by three main elements: nodes, ways (connected nodes), and relations (connected ways). These elements are tagged with one or more attribute keys that specify the element type. The keys belong to one of 29 feature classes e.g. building, highway, or land-use, which can then be specified in more detail by further attributes. In addition, elevation data is incorporated from the European Digital Elevation Model (EUDEM). Further, historical weather information is collected from `WorldWeatherOnline`.

For the application of the proposed approach, information about the transmit power P_{TX} is needed, which is usually not publicly available. Inspired by [4], we determine an estimation for $\tilde{P}_{\text{TX}}$ by curve fitting the log-distance model from [2] to the real world measurements (cf. Fig. 2 A). This is done once for every distinct scenario covered in the data.

B. Feature Engineering

Channel Features $\mathbf{x}_{\text{com}}$: For each transmitter-receiver pair, we determine the maximum first Fresnel zone width. Note that the n-th Fresnel zone radius F_n is defined by the following equation [2]:

$$F_n = \sqrt{\frac{n\lambda d_{\text{RX}} d_{\text{TX}}}{d_{\text{DP}}}} \quad (2)$$

where λ is the wavelength, d_{RX} and d_{TX} are the distances from the receiver and transmitter to the point of interest, and

d_{DP} is the Direct Path (DP)'s distance with $d_{\text{DP}} = d_{\text{RX}} + d_{\text{TX}}$. Further channel features utilized are an estimation of the path loss L based on the log-distance model from [2], the carrier frequency f, the bandwidth B, the transmitter's tilt angle θ_{TX} and $\tilde{P}_{\text{TX}}$ (cf. Eq. 1).

Position Features $\mathbf{x}_{\text{pos}}$: For each transmitter-receiver pair the 2D distance, the difference in elevation, and the transmitter as well as receiver heights are taken into account.

Geospatial Features $\mathbf{x}_{\text{geo}}$: In addition, three Bounding Boxes (BBoxes) are defined for each transmitter-receiver pair:

- *DP BBox*: describes the DP region with a BBox based on the DP's 2D distance d_{DP} and the third Fresnel zone radius F_3 for $d_{\text{RX}} = d_{\text{TX}}$ leading to a bounding box size of $1.2d_{\text{DP}} \times 10F_3$.
- *RX BBox*: describes the receiver region utilizing a $300 \times 300\,\text{m}$ BBox around the receiver position $\mathbf{p}_{\text{RX}}$ pointing towards the transmitter, based on [4].
- *TX BBox*: describes the transmitter region utilizing a $300 \times 300\,\text{m}$ BBox around the transmitter position $\mathbf{p}_{\text{TX}}$ pointing towards the receiver.

An example of these BBoxes is given in Fig. 3. For each BBox, numerical features are extracted. Fig. 2 B gives an overview of the different types incorporated in this process. Based on the OSM data the number of trees and buildings in the Region of Interest (RoI), the area covered by the buildings, the building's mean height, and its standard deviation are derived. Further, the areas of various land-use categories are extracted:

- *Developed Land*: e.g. Commercial, Residential, Industrial
- *Rural and Agricultural Land*: e.g. Grassland, Forest
- *Water Body*: e.g. River, Coastline, Wetland
- *Other Land*: e.g. Rock, Dune, Military

Finally, elevation-related features are inferred, including the difference between maximum and minimum elevation, and the elevation standard deviation. Taking into account geospatial features of the propagation environment and its surroundings allows not only an implicit classification of the propagation environment but also to learn the effects of obstacles on the wave propagation.

Weather Features $\mathbf{x}_{\text{wth}}$: According to [14], it is of necessity to calculate the attenuation caused by rain based on the rain amount. The authors in [15] study these effects together with the impact of humidity, pressure, and temperature. To take these effects into account, we utilize historical weather information including UV index, temperature, humidity, pressure, wind speed and direction, rain precipitation, and snowfall rate.

C. Machine Learning

The resulting feature vector $\mathbf{x} = [\mathbf{x}_{\text{com}}, \mathbf{x}_{\text{pos}}, \mathbf{x}_{\text{geo}}, \mathbf{x}_{\text{wth}}]$ holds 47 variables that are used to train various lightweight ML regressors. The latters' performance is evaluated based on the Root Mean Squared Error (RMSE) of the test data. These include a k-Nearest Neighbors (kNN) regressor, which is an instance-based learning technique, where predictions are not made based on an explicitly trained model, but based on the k most similar samples from the training data. The similarity of the data points is defined by their distance. The predicted values are then estimated based on an average of the considered samples [16].

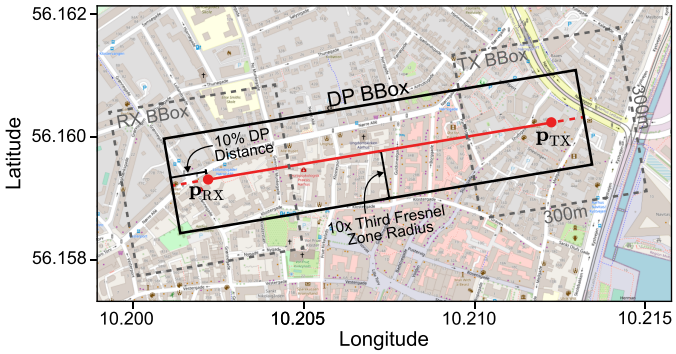

(a) Example for the city of Aarhus

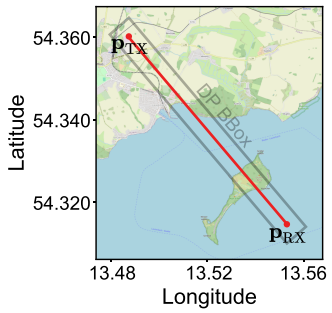

(b) Example for the baltic sea

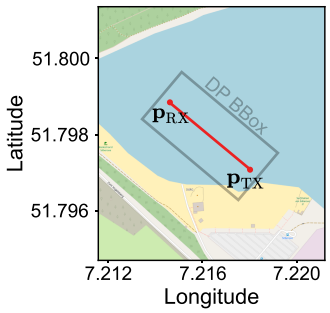

(c) Example for Haltern

Fig. 3. Visualization of the considered Bounding Box types for one receiver-transmitter pair in each scenario. (Map data: © OpenStreetMap Contributors, CC BY-SA)

Further, various tree-based regressors are investigated. The most basic type is a Decision Tree (DT), which represents a sequence of binary decisions in a tree-like structure. Each internal node represents a feature-based decision, while a leaf node represents the prediction value [16]. Random Forests (RFs) are ensemble methods that combine multiple uncorrelated DTs, where each DT only considers a subset of the dataset and features within each node [17]. Moreover, variants of gradient-boosting learning techniques are considered. Compared to classic RFs, tree-boosting algorithms build the series of DTs iteratively. We apply eXtreme Gradient Boosting (XGB) implementations by [18], where the DTs grow level-wise. In contrast, Light Gradient Boosting Machine (LGBM), introduced in [19], implements leaf-wise growth. Categorical Boosting (CatBoost) implementation by [20] comes with unique features such as symmetric trees and ordered boosting.

In addition, we consider Artificial Neural Networks (ANNs) [21]. The latters consist of multiple neurons arranged in layers and linked with weighted connections. Compared to tree-based learners, ANNs can model complex, non-linear relationships in data more effectively.

IV. Methodology

Evaluation scenarios: To investigate the performance of the proposed approach, we consider UAV measurements from

TABLE I
OVERVIEW OF THE COMPUTATIONAL EFFICIENCY AND TEST RMSE VALUES FOR DIFFERENT ML REGRESSORS AND DATA AGGREGATION METHODS.

Method	Prediction RMSE on Test Data [dB]						Computational Efficiency		
	Global			Cross-Scenario			Training	Test	Model
	Aarh.	Peen.	Halt.	Aarh.	Peen.	Halt.	Duration [s]	Duration[s]	Size [MB]
kNN	2.88	10.08	2.49	10.27	16.82	16.28	-	534.755	95.65
DT	3.34	9.37	3.12	10.30	20.17	15.97	7.333	0.014	0.13
RF	3.16	9.30	2.93	10.18	18.95	14.91	51.620	0.202	12.52
XGB	2.96	9.77	2.29	10.19	18.73	15.95	46.388	0.142	12.09
CatBoost	2.83	9.59	2.37	10.62	16.50	14.73	39.046	0.126	4.19
LGBM	2.71	9.29	2.45	10.07	18.82	16.44	7.440	0.149	6.91
ANN	3.46	6.44	5.17	29.91	19.26	17.58	845.530	1.531	0.36
Log-Distance	8.59	22.06	12.17	8.58	22.04	12.25	-	0.008	-

best performance second best performance
Note that log-distance predictions serve as an empirical benchmark.

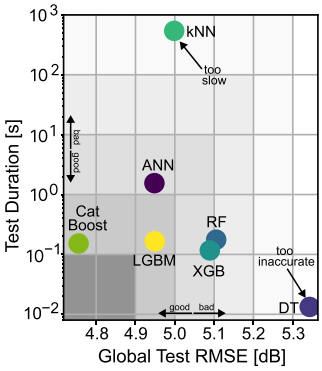

Fig. 4. Comparison of the regressors test duration and performance.

three distinct scenarios:

- *Haltern am See* (Germany) [22]: 41,240 data points were collected in flight heights up to 120 m in a rural and maritim environment (cf. Fig. 3c), where a private communication network was utilized.
- Region of *Peenemünde* (Germany) [23]: 181,185 data points, located at the baltic sea (cf. Fig.3b), were recorded over 16 experiments in private as well as public networks with flight heights up to 700 m. As the d_{DP} reaches values of over 40 km, samples for which d_{DP} exceeds 5 km are eliminated, leaving 76,216 samples.
- *Aarhus* (Denmark) [8]: 255,725 data points were recorded over 15 experiments in an urban environment (cf. Fig. 3) using a public network in flight heights from 10 to 100 m.

Validation methods: In order to quantify the performance of the proposed method, several benchmark models are included for validation. We take into account conventional models such as Friis free-space propagation and the two-ray ground-reflection model. Further we consider several UAV-specific models, namely 3GPP UMa and RMa [7], log-distance fit from [2], and ABG fit from [10]. Lastly, we apply the ML-driven DRaGon model [4] that is trained solely on G2G data.

Machine Learning methods: The ML evaluations are performed mainly with `scikit-learn`. For general training, the aggregated data set is shuffled and then split into 80% training and 20% testing data. The gradient-boosting algorithms are applied with the help of the corresponding Python libraries, namely `xgboost`, `catboost`, and `lightgbm`. ANN evaluations are performed by utilizing `PyTorch`. For hyperparameter tuning we perform so-called Bayesian optimization with the help of `wandb` toolkit.

V. RESULTS

A. Regression Model Selection

In order to gain first insight into what kind of ML regressors are suitable for Aerial-DRaGon, we make a performance comparison for the previously mentioned lightweight ML models. To fairly compare the results, all ensemble methods are limited to a total of 100 DTs, while the maximum depth of all DTs is set to 16 and the maximum number of leaf nodes is set to 1000. The studied kNN uses $k = 10$ neighbors. We also investigate the performance of a simple ANN with five hidden layers (64, 128, 256, 128, and 64 neurons per layer), which is trained for 100 epochs using a learning rate of 10^{-4}, a weight decay factor of 10^{-4}, a batch size of 256, and a dropout rate of 10%. In addition, early stopping is enabled, and a learning rate scheduler is applied. Therefore, 10% of the training data is used as a validation set. All other regressors' hyperparameters are using the default values provided.

Tab. I gives an overview of the achieved prediction RMSE values on the respective test data. There, two different data aggregation methods are examined. This includes a *global* approach, where the model is trained and tested on aggregated and shuffled data, and a *cross-scenario* evaluation, where the scenario under investigation is used as test data, while the remaining data is used for the training process.

The results for the *global* approach are very comparable across the regressors. It is striking that the poorest prediction accuracy is always achieved on the *Peenemünde* data, whereas the models deliver significantly lower RMSE values on *Aarhus* and *Haltern* data. While the ANN performs worst for the latter two, it is by far the most accurate in terms of *Peenemünde*. In general, it can be said that the RFs perform better than the classic DT, whereby the gradient-boosted variants CatBoost and LGBM tend to perform best. Even though all considered ML models outperform the empricial benchmark for all *global* evaluations, their prediction accuracies are worse for *Aarhus* and *Haltern* in *cross-scenario* context. However, the trend continues that the gradient boosting algorithms CatBoost and LGBM perform strongest in total. Nonetheless, the classic RF yields a comparatively good performance here.

In addition, the computational efficiency is analyzed in terms of training and test duration together with the saved model size, when trained on 298,585 and evaluated on 74,574 samples. To have a fair comparison, all models are tested using the same hardware limitations. Solely the ANN is trained GPU-accelerated, while the remaining models are trained under the same conditions under which they are tested. In terms of computational efficiency, the DT performs best, as

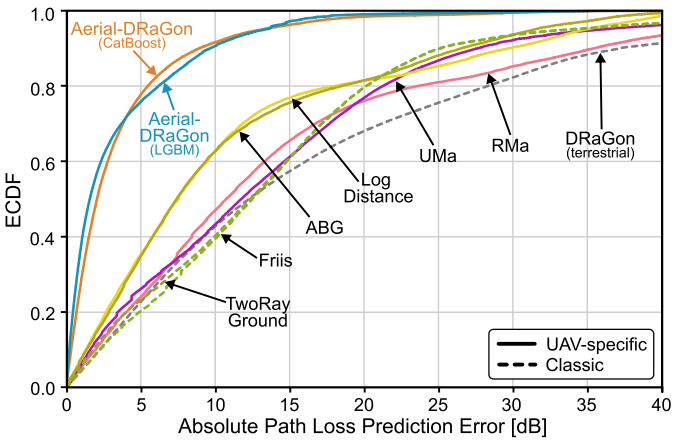

Fig. 5. Comparison of Aerial-DRaGon together with benchmark models evaluated on real-world measurements.

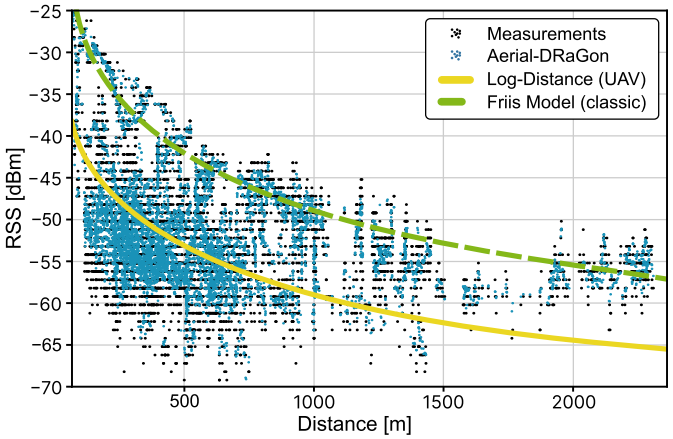

Fig. 6. Measured and predicted values of the Aerial-DRaGon together with analytical models plotted over the distance.

it has the fastest training, testing, and smallest model size. While kNN algorithm does not have any model parameters to be trained, it comes up with a heavy time for evaluating new data, which can also be recognized in Fig. 4 that shows the *global* test RMSE plotted against the test duration. It can be noted here too that CatBoost and LGBM perform best.

B. Hyperparameter Tuning

Further, we perform hyperparameter tuning for both LGBM and CatBoost, as they yield good performance in general as the above analysis shows. We perform bayesian optimization in a *cross-scenario* manner, as Tab. I revealed that this is particularly challenging. Therefore, we use a subset of *Aarhus* and *Peenemünde* data for training, and a subset of *Haltern* for validation. Based on the results of the automated tuning, we manually fine-tuned the configurations. The final selected hyperparameter combinations are displayed in Tab. II. For both methods more than 1200 combinations over eight hyperparameters were analyzed.

C. Performance Comparison and Validation

To compare the proposed method with the reference channel models, we use an Empirical Cummulative Distribution Function (ECDF) of the absolute prediction error, which can be seen in Fig. 5. Both selected ML regressors (see subsection V-A) are trained in a *global* manner. The remaining, unseen 20% of the aggregated data are utilized as test data for evaluating the ML and reference models.

TABLE II
SELECTED HYPERPARAMETERS FOR CATBOOST AND LGBM.

Hyperparameter	**CatBoost**	**LGBM**
Number of Trees	120	100
Maximum Depth	10	45
Maximum Leaf Number	-	3,500
Learning Rate	0.3	0.15
Minimum number of data needed in a child	40	40
Booster	Plain	GBDT
Grow Policy	SymmetricTree	-
Subsample Ratio of the Training Instances	0.65	0.65
Subsample Ratio of columns when construction each tree	-	0.65
Subsample Ratio of columns for each level	0.6	-

It can be seen that both Aerial-DRaGon variants outperform all the reference models by having RMSE values of 5.91 dB for LGBM and 6.07 dB for CatBoost, respectively. The best reference models in terms of prediction accuracy are the ABG fit proposed in [10] with 14.48 dB and the log-distance fit from [2] with 15.40 dB RMSE. Besides the 3GPP RMa model, the remaining analytical channel models yield similar, but slightly worse accuracies with RMSE values between 16.85 dB and 17.38 dB. The 3GPP RMa only achieves 21.80 dB RMSE and is therefore significantly less accurate than the UMa variant, which is likely due to the fact that the test data consists of more urban than rural samples. This performance is only slightly better than the one achieved by the DRaGon model - more precisely 21.46 dB RMSE - that is trained solely on G2G communication data and consequently did not learn a height dependency of the path loss. Due to its better performance, Aerial-DRaGon s LGBM variant is used exclusively below.

In order to investigate why the predictions of the benchmark models are significantly less precise, we want to provide a deeper insight with the help of Fig. 6. The latter shows the measured values together with the predictions of the *global* trained Aerial-DRaGon over the distance. Here, the *Aarhus* test data with a carrier frequency of 1870 MHz and 30 m UAV height is utilized. Further, Friis propagation and log-distance fit from [2] serve as a reference. It should be noted, that all methods achieve significantly lower RMSE values of 2.70 (Aerial-DRaGon), 8.58 (log-distance), and 13.98 dB (Friis) on the *Aarhus* data.

Overall, it can be observed that the measured RSS values are highly scattered. While Aerial-DRaGon can replicate the measurements properly, they are poorly captured by classic large-scale models, resulting in low prediction accuracies for most of the reference models. By adding stochastically modeled

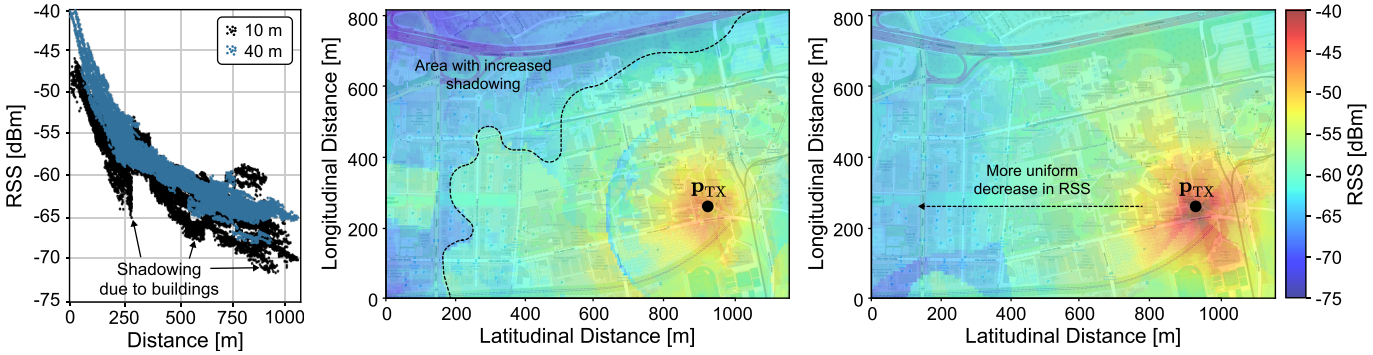

(a) RSS values over the distance (b) Predicted RSS REM for 10 m receiver height (c) Predicted RSS REM for 40 m receiver height

Fig. 7. Analysis of the predictions of Aerial-DRaGon trained on the Aarhus data and exploited on an unknown urban scenario for different receiver heights.

shadow fading, the dispersion of the measurement data can be mimicked, but the accuracy in predicting the path loss for a specific transmitter-receiver pair remains poor. Furthermore, it is evident that Friis propagation is too optimistic meaning it assumes a too low path loss. This behavior is to be expected assuming that ideal conditions are modeled here, which do not occur in reality.

D. Height-dependent REM Generation

As pointed out in Sec. I, height-dependent REMs can be a key enabler for cooperating air taxis. Consequently, we utilize Aerial-DRaGon, trained on the *Aarhus* data, to generate REMs of TU Dortmund University for two receiver heights and one transmitter. The resulting REMs are shown in Fig. 7 for 10 m and 40 m height in addition to the complemented scatterplot of the predicted values over the distance. It can be observed that the predictions for the greater UAV height have a higher RSS level. Although, one would expect the RSS values to decrease with increasing receiver height due to the G2G-optimized base stations, [7] points out that UAVs observe higher RSSs than receivers close to the ground, but the RSS decreases again above a certain height. The predictions in Fig. 7 can be explained by the fact that the receiver with 10 m height is below the average building level, which is closer to G2G than A2G conditions. In contrast, for a height of 40 m the LOS probability increases significantly, resulting in lower attenuations compared to 10 m height.

VI. Conclusion and Outlook

In this paper, we presented the novel ML-driven Aerial-DRaGon path loss prediction method for non-static aerial systems that exceed the height limitations of classic propagation models. As demonstrated in our comprehensive performance evaluation, the proposed model outperforms classic as well as UAV-specific channel models by difference in RMSE of at least 8.57 dB. While Aerial-DRaGon achieves very accurate predictions in a *global* manner, the transferability of Aerial-DRaGon for scenarios, which differ considerably from the training data, can be enhanced in future work. The latter can be carried out by adding further data sets to the training process.

In addition, we plan to employ the model on an UAV platform, where software- and hardware-level optimization in the manner of TinyML [24] is planned to meet the systems hardware constraints and reduce the model's energy requirements as much as possible.

This also offers the possibility to use the model in the context of communication-aware trajectory planning (cf. Fig. 1). Current work in this field, such as [25], already focuses on communication-aware trajectory planning for UAVs in Non-Terrestrial Networks (NTNs). By integrating novel A2G channel models like Aerial-DRaGon into the proposed digital twin, we plan to extend the trajectory planning to lower airspace networks, allowing for multi-network and multi-technology awareness.

Acknowledgment

This work has been supported by the German Federal Ministry of Education and Research (BMBF) in the course of the 6GEM research hub under grant number 16KISK038 and the project LARUS-PRO under grant number 14N15666. It is further supported by the project DRZ (Establishment of the German Rescue Robotics Center) under funding reference 13N16476.

We would like to thank the Wireless Communication Networks Institute at Aalborg University for providing the measurement data collected in the city of Aarhus.

References

[1] 5GAA, "Making 5G proactive and predictive for the automotive industry," 5G Automative Association, Tech. Rep., Dec 2019.

[2] R. Amorim, P. Mogensen, T. Sorensen, I. Z. Kovacs, and J. Wigard, "Pathloss measurements and modeling for UAVs connected to cellular networks," in *2017 IEEE 85th Vehicular Technology Conference (VTC Spring)*, 2017, pp. 1–6.

[3] J. Won, D.-Y. Kim, Y.-I. Park, and J.-W. Lee, "A survey on UAV placement and trajectory optimization in communication networks: From the perspective of air-to-ground channel models," *ICT Express*, vol. 9, no. 3, pp. 385–397, 2023.

[4] B. Sliwa, M. Geis, C. Bektas, M. López, P. Mogensen, and C. Wietfeld, "DRaGon: Mining latent radio channel information from geographical data leveraging deep learning," in *2022 IEEE Wireless Communications and Networking Conference (WCNC)*, 2022, pp. 2459–2464.

[5] M. Geis, B. Sliwa, C. Bektas, and C. Wietfeld, "TinyDRaGon: Lightweight radio channel estimation for 6G pervasive intelligence," in *2022 IEEE Future Networks World Forum (FNWF)*, Montreal, Canada, Oct. 2022, Best Paper Award.

[6] 3GPP, "5G; Study on channel model for frequencies from 0.5 to 100 GHz," 3rd Generation Partnership Project (3GPP), Technical Report (TR) 38.901, Apr 2022, version 17.0.0 Release 17.

[7] ——, "Study on enhanced LTE support for aerial vehicles," Technical Report (TR) 36.777, Dec 2017, version 15.0.0 Release 15.

[8] M. Bucur, T. Sorensen, R. Amorim, M. Lopez, I. Z. Kovacs, and P. Mogensen, "Validation of large-scale propagation characteristics for UAVs within urban environment," in *2019 IEEE 90th Vehicular Technology Conference (VTC2019-Fall)*, 2019, pp. 1–6.

[9] R. Amorim, H. Nguyen, P. Mogensen, I. Z. Kovács, J. Wigard, and T. B. Sørensen, "Radio channel modeling for uav communication over cellular networks," *IEEE Wireless Communications Letters*, vol. 6, no. 4, pp. 514–517, 2017.

[10] Y. Lv, Y. Wang, J. Chai, and W. Wang, "Ultra wideband channel measurement and analysis for low altitude UAV air-to-ground scenario," in *2021 13th International Symposium on Antennas, Propagation and EM Theory (ISAPE)*, vol. Volume1, 2021, pp. 1–3.

[11] N. Goddemeier, K. Daniel, and C. Wietfeld, "Coverage evaluation of wireless networks for unmanned aerial systems," in *2010 IEEE Globecom Workshops*, 2010, pp. 1760–1765.

[12] ——, "Role-based connectivity management with realistic air-to-ground channels for cooperative UAVs," *IEEE Journal on Selected Areas in Communications*, vol. 30, no. 5, pp. 951–963, 2012.

[13] A. Seretis and C. D. Sarris, "An overview of machine learning techniques for radiowave propagation modeling," *IEEE Transactions on Antennas and Propagation*, vol. 70, no. 6, pp. 3970–3985, 2022.

[14] ITU, "Specific attenuation model for rain for use in prediction methods," Report, Sep 2005.

[15] H. B. Hamid Dutty and M. M. Mowla, "Weather impact analysis of mmWave channel modeling for aviation backhaul networks in 5G communications," in *2019 22nd International Conference on Computer and Information Technology (ICCIT)*, 2019, pp. 1–6.

[16] C. M. Bishop, *Pattern Recognition and Machine Learning (Information Science and Statistics)*. Berlin, Heidelberg: Springer-Verlag, 2006.

[17] L. Breiman, "Random forests," *Mach. Learn.*, vol. 45, no. 1, pp. 5–32, Oct 2001.

[18] T. Chen and C. Guestrin, "XGBoost: A scalable tree boosting system," in *Proceedings of the 22nd ACM SIGKDD International Conference on Knowledge Discovery and Data Mining*, ser. KDD '16. New York, NY, USA: Association for Computing Machinery, 2016, p. 785794.

[19] G. Ke *et al.*, "LightGBM: A highly efficient gradient boosting decision tree," in *Advances in Neural Information Processing Systems*, vol. 30. Curran Associates, Inc., 2017.

[20] L. Prokhorenkova, G. Gusev, A. Vorobev, A. V. Dorogush, and A. Gulin, "CatBoost: Unbiased boosting with categorical features," in *Proceedings of the 32nd International Conference on Neural Information Processing Systems*, ser. NIPS'18. Red Hook, NY, USA: Curran Associates Inc., 2018, p. 66396649.

[21] I. Goodfellow, Y. Bengio, and A. Courville, *Deep Learning*. MIT Press, 2016, http://www.deeplearningbook.org.

[22] J. Tiemann, O. Feldmeier, and C. Wietfeld, "Supporting maritime search and rescue missions through UAS-based wireless localization," in *2018 IEEE Globecom Workshops (GC Wkshps)*, 2018, pp. 1–6.

[23] J. Güldenring *et al.*, "Reliable long-range multi-link communication for unmanned search and rescue aircraft systems in beyond visual line of sight operation," *Drones*, vol. 4, no. 2, 2020.

[24] M. Shafique, T. Theocharides, V. J. Reddy, and B. Murmann, "Tinyml: Current progress, research challenges, and future roadmap," in *2021 58th ACM/IEEE Design Automation Conference (DAC)*, 2021, pp. 1303–1306.

[25] T. Gebauer, F. Weißberg, and C. Wietfeld, "COMPASS: Communication-aware Trajectory Planning for UAV-based Rescue Missions via Non-Terrestrial Networks," in *2024 IEEE 99th Vehicular Technology Conference (VTC-Spring)*, Jun. 2024.